Properties of radiating pointlike sources in cylindrical omnidirectionally reflecting waveguides

Peter Bermel, J. D. Joannopoulos, and Yoel Fink
Center for Materials Science and Engineering and Institute for Soldier Nanotechnologies, Massachusetts Institute of Technology, Cambridge, Massachusetts 02139, USA

Paul A. Lane and Charles Tapalian
Charles Stark Draper Laboratory, Cambridge, Massachusetts 02139, USA
(Received 22 July 2003; published 23 January 2004)

The behavior of pointlike electric dipole sources enclosed by an axially uniform, cylindrically symmetric waveguide of omnidirectionally reflecting material is analyzed. It is found that the emission spectrum of a source inside the waveguide is strongly modified by features resembling one-dimensional Van Hove singularities in the local density of states (LDOS). Additionally, *more* than 100% of the power radiated by a dipole in vacuum can be captured at the end of the waveguide, owing to the overall enhancement of the LDOS (the Purcell effect). The effect of varying the positions and orientations of electric dipole sources is also studied.

DOI: 10.1103/PhysRevB.69.035316 PACS number(s): 42.70.Qs, 42.79.Gn

I. INTRODUCTION

A variety of technologically significant devices rely on guiding light from a source placed inside a waveguide. These include optical amplifiers, which utilize index guiding, and hollow waveguide sensors, which confine light with metal or high-index material. While the guiding mechanisms in these two devices are different, both exhibit low output efficiency and may be limited by the core material properties. With the index-guiding mechanism, isotropic emission from a randomly oriented collection of dipoles leads to high radiation losses. In the case of metal, high ohmic losses occur at IR and visible wavelengths.[1–3]

Rather than using lossy metallic structures, one could also envision using a highly reflective dielectric mirror to confine light. In this paper we study the performance of a structure consisting of a uniform index core, possibly air, surrounded by a dielectric mirror cladding, known as an omniguide. We find that this structure not only minimizes the losses due to radiation and absorption, but due to the Purcell effect, also achieves an output power that exceeds that of the source in vacuum at some frequencies.

It has been known for some time that a finite slab of stratified dielectric media will reflect certain frequencies of light better than others. One could easily predict multiple slabs of dielectric could enhance this effect for a target frequency. However, solving any but the simplest of cases is a formidable problem using the method of multiple reflections.[4] Nonetheless, the development of the transfer-matrix method by multiple authors in the 1940s and 1950s led to the theoretical prediction of highly efficient dielectric mirrors.[5–7] This approach was then extended to the cylindrical case by Yeh and Yariv in 1978.[8] Although the theory developed by Yeh and Yariv is of general applicability, emphasis was placed on obtaining Bragg reflections for a specific frequency and conserved wave vector, which could be obtained using a relatively small dielectric contrast. In early papers, for example, Cho, Yariv, and Yeh conducted experiments on Bragg waveguides with a reflecting layer of indices $n_1=3.43$ and $n_2=3.35$;[9] Yeh considered a slightly higher contrast of $n_1=2.89$ and $n_2=3.38$ in a theoretical paper.[10] However, other studies indicated that ten layers of a low dielectric-contrast cladding (with $n_1=1.485$ and $n_2=1.45$) for a hollow-core structure, even with a radius of tens of wavelengths, can result in losses in excess of 1 dB per mm.[11] The benefits of using a high-contrast periodic dielectric fiber ($n_1=4.0$, $n_2=2.4$) with metal on the outside was also studied theoretically,[12] but to the best of our knowledge, not implemented experimentally. As a result, most studies of these Bragg fibers continued to focus on low-contrast dielectric claddings through the mid 1990s, despite their limitations.[13] Interest in these structures was renewed, however, upon the theoretical discovery and experimental fabrication of omnidirectional mirrors—one-dimensionally periodic dielectric structures that reflect light from all incident angles and polarizations.[14] The concept of omnidirectional reflectivity can readily be extended to a system with cylindrical symmetry.[15–17] Recently, these structures have been fabricated in fiber form and used to demonstrate low-loss transmission of high-intensity IR light.[18,19]

The behavior of pointlike light sources in an omniguide is an interesting problem for two reasons: spontaneous emission may be modified and coupling to index-guided modes may occur. Spontaneous emission will take place in the photon modes available to the emitter. All the electromagnetic modes of free space are not necessarily available in the presence of materials. For example, it has been shown theoretically and experimentally that a pointlike light source between two conducting plates will experience strongly suppressed emission below the cutoff frequency.[20,21] Also, it has been shown experimentally[22] that a metallodielectric photonic crystal suppresses spontaneous emission at frequencies within the band gap, giving rise to emission concentrated within a relatively narrow frequency range. In this work, the hollow cylindrical core mimics a line defect in a three-dimensional (3D) photonic crystal structure. We operate at frequencies within the gap, where most photon modes are suppressed except for those associated with the hollow-core defect. Spontaneous emission into these hollow-core modes would be predicted to be strongly enhanced. The sec-

ond issue regards coupling to index-guided modes. A monochromatic pointlike light source in a hollow waveguide can couple to modes at a given frequency with any axial wave vector, i.e., values both above and below the light line. The modes below the light line are evanescent and would not cause losses in equilibrium if the waveguide were made of perfect conductor; however, in a hollow waveguide with dielectric cladding, fields that are evanescent inside the hollow core can couple to propagating modes in the dielectric cladding. These index guided modes can be lossy if the material outside the dielectric cladding has an index higher than the hollow core, or if there are any bends or kinks in the dielectric cladding.

The behaviors of pointlike light sources in artificial opals and 2D triangular lattices of rods have been predicted through the calculation of the local density of states at several points within the systems.[23] Also, Green's function of a point source in an optical waveguide has been calculated in two dimensions.[24] However, the behavior of light sources in 1D periodic hollow omniguide structures has yet to be explored in detail.

This paper pursues the problem in several steps. First a realistic model of an omniguide fiber, suitable for simulation, is developed. Initial results for a single dipole at the center of the omniguide, which indicate a substantial modification of the rate of spontaneous emission in vacuum, are then presented. They are explained in terms of the local density of states of the 1D omniguide system. Additional results for dipoles with different radial positions and orientations are then given. Finally, the problem of a dipole at the inner surface coupling to index-guided modes in the cladding is discussed.

II. SIMULATION

The computational setup is illustrated to scale in Fig. 1. Following Ref. 16, the high-index tellurium (Te) layers ($n=4.6$) have a thickness one-half that of the low-index polystyrene (PS) layers ($n=1.6$); the thickness of one Te/PS bilayer is defined as a. The inner radius of the hollow core, r_i, defined as the distance from the center of the cylinder to the first layer of dielectric material, is chosen to be $2.144a$. For a realistic set of materials such as titania and silica, one might require 20 bilayers; for computational ease, three layers of tellurium and polystyrene, materials used for experiments in infrared in Ref. 14, are substituted. Therefore, the outer radius r_o defined as the distance from the center of the cylinder to the outer air region is $5.144a$.

A single dipole source is placed at one end of the waveguide within the hollow-core region. In the limit of an infinite number of layers of an omnidirectionally reflecting mirror, all of the emitted light should presumably couple into lossless propagating modes. The actual number of layers required for relatively high reflection is illustrated in Fig. 2.

For this system, Maxwell's equations are solved in a finite difference time-domain simulation, based on the work of Yee,[25] using perfectly matched layer absorbing boundary conditions.[26] A constant-frequency ac current modulated by a Gaussian envelope serves as the electric dipole source. The

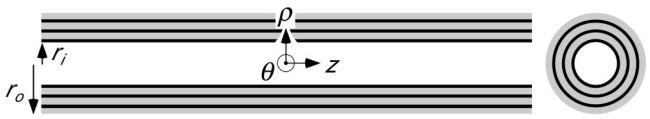

FIG. 1. Waveguide used in simulations, consisting of three bilayers of tellurium ($n=4.6$) and polystyrene ($n=1.6$). The core is hollow and made of air (the inner radius—the distance from the center to the innermost cladding layer—is given by $r_i=2.144a$; the outer radius—the distance from the center to the outermost cladding layer—is given by $r_o=5.144a$).

key quantity of interest is the total flux emerging from the far end of the waveguide, which is measured in the simulation as the integrated Poynting flux through a square plane covering the hollow-core region.

III. RESULTS AND DISCUSSION

While there are many possibilities for the placement and orientation of even a simple dipole current source, we start off with it placed at one end of the waveguide in the center of the hollow region. There are still many choices for the orientation of the dipole; we choose a dipole pointing along

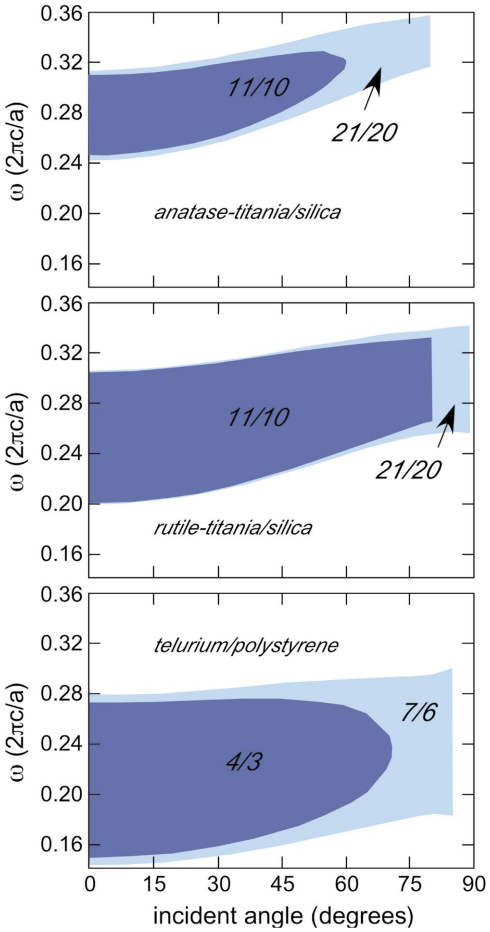

FIG. 2. (Color) Illustration of the −20-dB transmission ranges (i.e., for which at least 99% of light is reflected) for two different thicknesses (first number is the number of high-index layers, second number is the number of low-index layers).

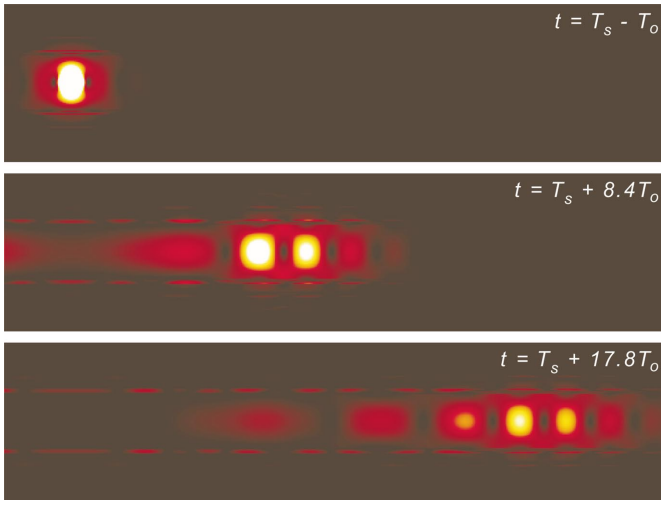

FIG. 3. (Color) Snapshots of the distribution of electrical power in the waveguide for a single dipole at the center of the hollow core. Times are given here and in other figures relative to the time of peak emission, T_s, in units of the period of the central frequency, T_o.

the axial direction z since in vacuum, it would lose most of its power in the transverse directions, leaving very little at a small flux plane far away in the z direction. The introduction of a cylindrical dielectric mirror changes this result dramatically, however. In Fig. 3, the initial dipole pulse encounters the reflective wall and couples into the TM_{01} mode, which propagates down the hollow part of the waveguide and leaves the far end. Figure 4 quantifies the effect of the presence of the waveguide, by measuring the frequency spectrum of the flux in arbitrary units [defined as $F(\omega)=\int_{\text{surface}}\mathbf{S}(\omega)\cdot\hat{\mathbf{n}}dA$, where $\mathbf{S}(\omega)=\frac{1}{2}\text{Re}\{\mathbf{E}(\omega)\times\mathbf{H}(\omega)^*\}$, and $\mathbf{E}(\omega)=\int_0^T e^{i\omega t}\mathbf{E}(t)dt$, etc.) and comparing it to the flux observed for a hollow glass waveguide and the total flux emitted by a dipole in vacuum.

Clearly, the performance of a hollow glass tube ($n=2.6$), which relies upon index guiding, is several orders of magnitude below the ideal of 50% transmission of the total flux emitted in vacuum. The hollow cylindrical waveguide,

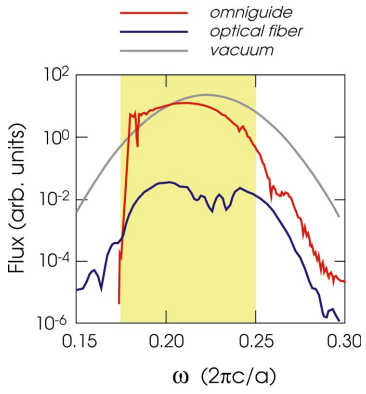

FIG. 4. (Color) Flux spectrum for a dipole at the center of the hollow core, plus data for a hollow glass fiber ($n=2.6$), and the total flux of the dipole in vacuum.

on the other hand, has enhanced performance vis-à-vis the vacuum case within a narrow range of frequencies above cutoff. This behavior is a result of the *Purcell effect*. Purcell found that boundary conditions on the electromagnetic field around a dipole emitter can substantially alter the emission rate.[27] In the case of a resonant cavity with a single resonant mode of quality factor Q, it has been shown[20] that the spontaneous rate of emission at the resonant frequency will be enhanced by a factor of Q. One can also make the more detailed calculation by first noting that the frequency near cutoff is given by $\omega^2=\omega_c^2+c^2k_z^2/n^2$, where ω_c is the cutoff frequency and k_z is the component of the wave vector pointing along the long axis, which yields the following expression for the density of states within the cavity:[20] $g_C(\omega)=(2/V)(dn/d\omega)=(4/cA_g)(\omega/\sqrt{\omega^2-\omega_c^2})$. Clearly this formula can be generalized to accommodate multiple modes with these types of singularities characteristic of one-dimensional periodicity (Van Hove-type singularities). To obtain a detailed comparison with time-domain simulations, however, the density of states, given formally by $g(\omega)=\Sigma_{n,k}\delta(\omega-\omega_{nk})$, was calculated numerically. The technique used involved a linear extrapolation of the eigenfrequencies calculated at a mesh of k points, as described by Gilat and Raubenheimer.[28] The global density of states calculation is difficult to interpret, since in addition to several peaks from the resonant modes, there are many others from nearly degenerate index-guided modes. In order to isolate the important features of this density of states calculation, we look at the photonic local density of states, which is defined here as $g_L(\omega,\mathbf{r})=\Sigma_{n,k}\epsilon(\mathbf{r})|\mathbf{E}_{nk}(\mathbf{r})|^2\delta(\omega-\omega_{nk})$, where the fields are normalized such that $\int d\mathbf{r}\epsilon(\mathbf{r})|\mathbf{E}_{nk}(\mathbf{r})|^2=1$, for all n and k, which implies we can recover the global density of states by integrating, $g(\omega)=\int d\mathbf{r}g_L(\omega,\mathbf{r})$.

The results obtained both at the center of the hollow cavity and at a distance 1.2 times the lattice spacing away from the center are shown in Fig. 5.

In this case, the greatly decreased density of states within the band gap below cutoff, and the enhanced density of states associated with the hollow-core resonant modes, leads to enhanced emission just above cutoff for modes to which the dipole can couple.

This behavior shows that a cylindrically symmetric, omnidirectionally reflective coating can create an environment in which dipole emitters can efficiently couple into low-loss resonant modes in the hollow core. In Fig. 6, a different pulse is used to show the behavior near cutoff in more detail. While the total integrated power $\int F(\omega)d\omega$ is greater for the dipole in the waveguide than in vacuum, that's not physically unreasonable since the conserved quantity in our simulations is simply the current, while power is given by the current acting against the local field, which may be selectively enhanced at certain frequencies and positions in the presence of dielectric.

Next, we consider the behavior of a dipole close to the inner surface of the hollow tube (at $\rho=2a$, with $r_i=2.144a$). The flux spectrum for dipoles oriented in the ρ, θ, and z directions (see Fig. 1) are shown in Fig. 7. In Figs. 8–10, the redistribution of electric power as a function of

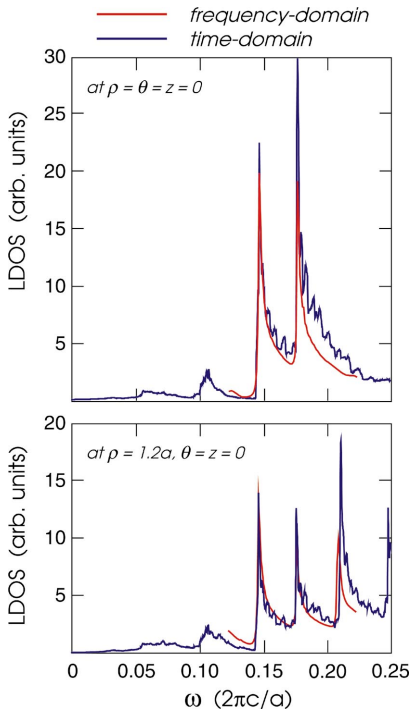

FIG. 5. (Color) Local electric density of states for the hollow cylindrical waveguide. Note the presence of sharp $1/\sqrt{\omega-\omega_c}$ type singularities, as predicted.

time is shown for these same three orientations. Performance varies dramatically with the orientation of the dipole. The presence of a sharp rise in the transmission at a certain frequency can be interpreted as a cutoff corresponding to a hollow-core guided mode. The lack of such a cutoff can generally be interpreted as a sign that any transmission would come through an index-guiding mechanism. Thus, we surmise that a dipole oriented along ρ will couple much more efficiently to the hollow-core guided modes than the dipoles pointing along θ or z. This interpretation is supported by the snapshots of the power distribution in Figs. 8–10. Furthermore, a circular flow of energy is observed for the dipole oriented along z, as illustrated in Fig. 11.

Also, the behavior of a dipole intermediate between the inner surface and center of the hollow tube in the transverse direction (at $\rho=1.2a$, with $r_i=2.144a$) is considered. In contrast with the previous results for a dipole situated adjacent to the inner surface (see Fig. 7), the dipoles oriented along θ and z in this middle position are able to couple to the hollow-core guided modes, as suggested by the presence of cutoffs in the flux spectra shown in Fig. 12. This is also illustrated more explicitly in Figs. 13–15, where all three orientations are shown coupling into these modes, in contrast with Figs. 8–10.

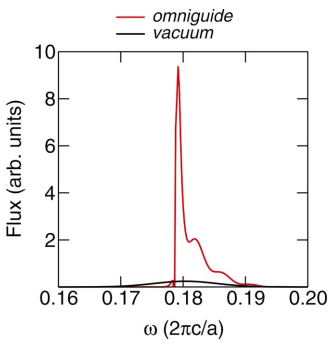

FIG. 6. (Color) Flux spectrum for a dipole at the center of the hollow core, as in Fig. 4, but zoomed in on the region near cutoff.

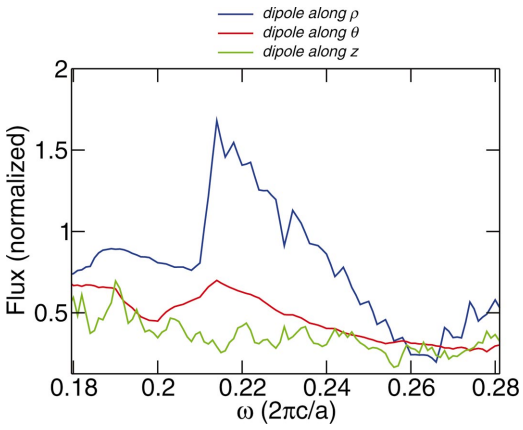

FIG. 7. (Color) Flux spectrum for dipoles on the inner surface of the hollow core, oriented in the ρ, θ, and z directions, normalized by the flux of a dipole in vacuum.

Evidently dipole sources near the inner-core radius can have strong coupling to modes which exist in the dielectric cladding. This is consistent with the finding that the local density of states of an omnidirectional reflector is not zero, or even small, but instead characteristic of a waveguide.[29] In other words, they are index-guided modes. However, empirically, it is observed that the coupling of dipoles to these modes is decreased if they are at a distance of order $\lambda/4$ away from the inner surface. This analysis suggests that a low-index coating may prevent coupling to the problematic index-guided modes. It may immediately be noted that as the index of the inner coating approaches unity, the performance should be the same as the case illustrated in Figs. 12 and

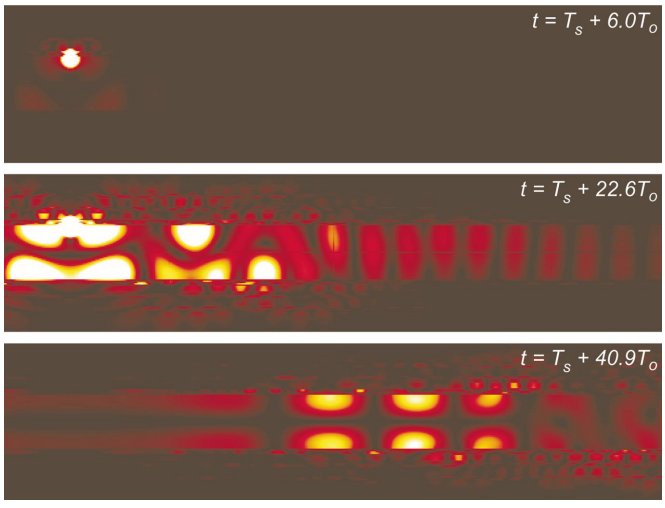

FIG. 8. (Color) Snapshots of the distribution of electrical power in the waveguide for a single-dipole source on the inner surface pointing in the ρ direction.

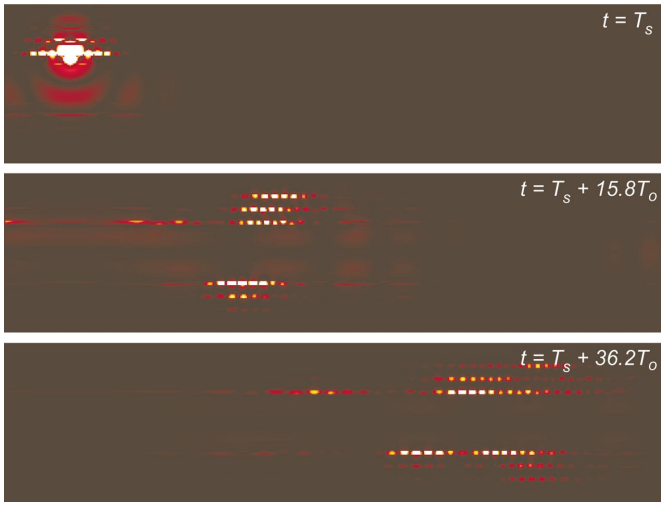

FIG. 9. (Color) Snapshots of the distribution of electrical power in the waveguide for a single-dipole source on the inner surface pointing in the θ direction.

13–15, since the inner coating would just act like an extension of the hollow core. However, the yield of a hollow tube with a "low-index" ($n=1.3$) coating which extends from $\rho=1.2a$ to $\rho=2.144a$ was also tested, and the result, as well as a comparison to the $n=1$ case, is given in Fig. 16. It is found that if one couples to the appropriate modes which have frequencies within the range of omnidirectional reflection, efficiencies comparable to the previous case of a dipole away from the surface, essentially suspended in air, can be achieved. The propagation of this mode is illustrated in Fig. 17.

Next, we calculate the dispersion of modes localized to the core. The dispersion of a wave packet with a relatively narrow range of frequencies is proportional to $d^2k_z/d\omega^2$ evaluated at the central frequency.[30] In terms of units useful for interpreting numerical calculations, the spatial separation accrued per unit frequency difference between waves per unit distance traveled along the waveguide, the dispersion is given by $D=(d\omega/dk_z)(d^2k_z/d\omega^2)$. It can be shown that for small k_z, which dominates the spontaneous emission spectrum, the dispersion is approximately proportional to the core index. This comes about from two competing effects. First, a lower group velocity decreases the spatial separation between nearby modes. However, a flatter band means there will be a greater spread of axial wave vectors. Since distance along the waveguide and frequency spread are held constant in the two simulations, the overall effect is an increase in the separation between modes in system with a low-index coating, as can be observed by comparing Figs. 3 and 17.

Finally, we discuss one potential application: a detector for fluorescent molecules. One could design the omniguide to be transparent at excitation frequencies, and reflective at emission frequencies. Then, ideally, the spontaneously emit-

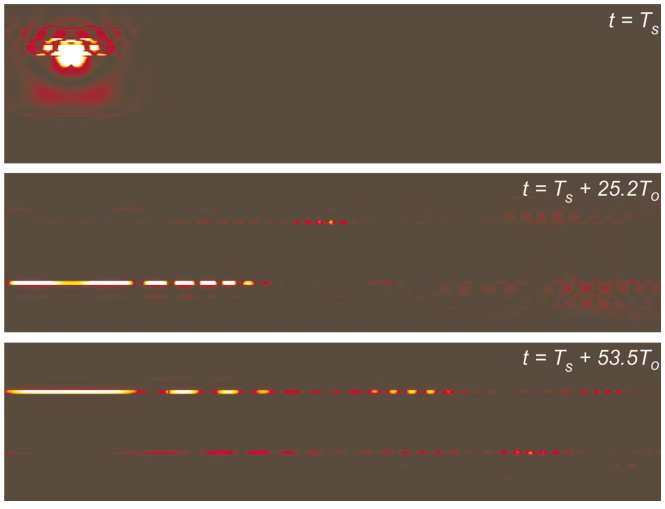

FIG. 10. (Color) Snapshots of the distribution of electrical power in the waveguide for a single-dipole source on the inner surface pointing in the z direction.

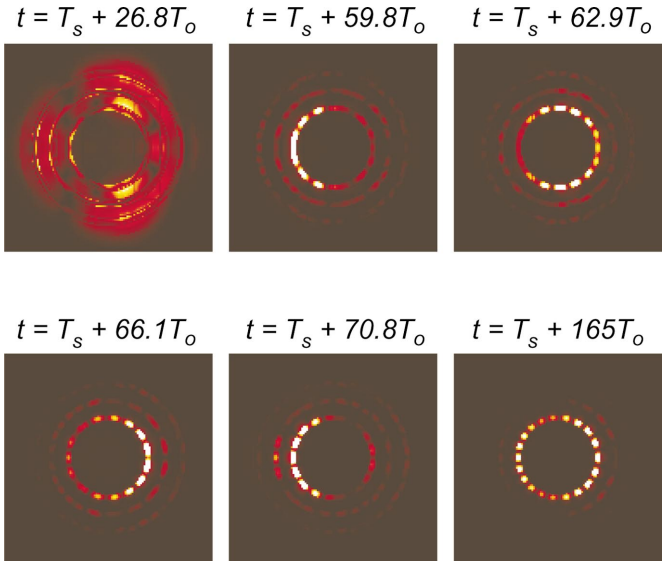

FIG. 11. (Color) Snapshots of the distribution of electrical power in a cross section of the waveguide away from the source which is located near the wall ($\rho=2a$, $r_i=2.144a$), and pointing along z.

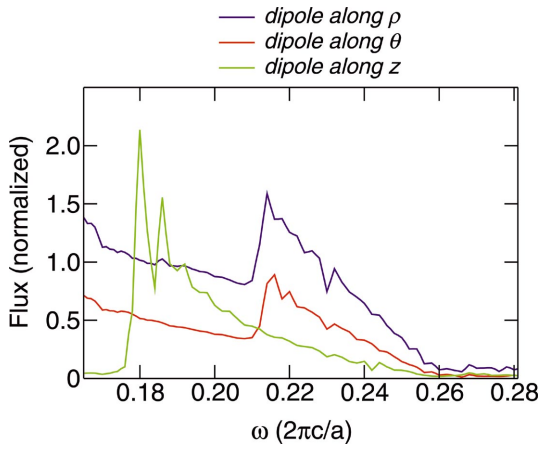

FIG. 12. (Color) Flux spectrum for dipole roughly halfway between the center and inner wall of the hollow core, i.e., at $\rho=1.2a$ ($r_i=2.144a$), normalized by the flux of a dipole in vacuum.

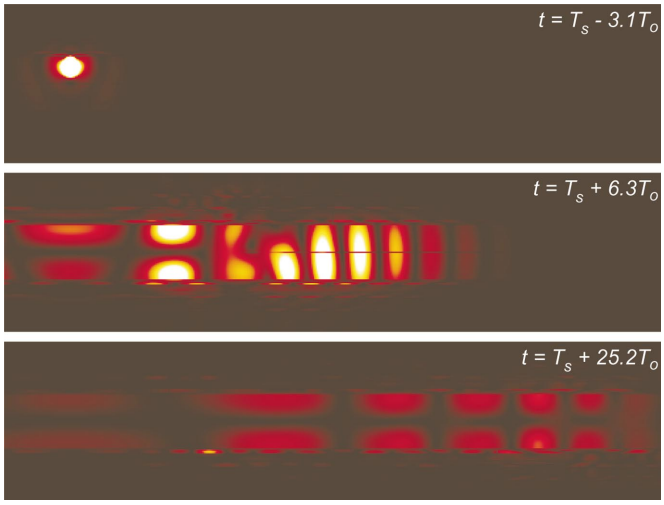

FIG. 13. (Color) Snapshots of the distribution of electrical power in the waveguide for a single-dipole source near the inner surface ($\rho = 1.2a$, $r_i = 2.144a$) pointing in the ρ direction.

ted radiation could only couple to hollow-core guided modes, which would propagate to the end of the waveguide with low losses. The important design considerations are as follows: making sure the fluorescent molecules do not couple to index-guided modes, choosing the core radius to control the available guided core modes, and choosing the number of layers to keep losses over the length of the omniguide acceptably low. The fluorescent molecules can be kept from coupling to index-guided modes by introducing a low-index coating, as discussed above. For an index-guided cladding mode near the light line, the damping factor over a distance x is given by $e^{-2\pi\sqrt{n_h^2 - n_c^2}(x/\lambda)}$, where n_h is the refractive index of the high-index cladding layer and n_c is the refractive index of the low-index coating. For $n_h = 4.6$, $n_c = 1.2$, $x = \lambda/4$, this factor is 0.1%, which shows that a thin coating is more than sufficient for high-contrast materials.

The considerations involved in choosing the appropriate

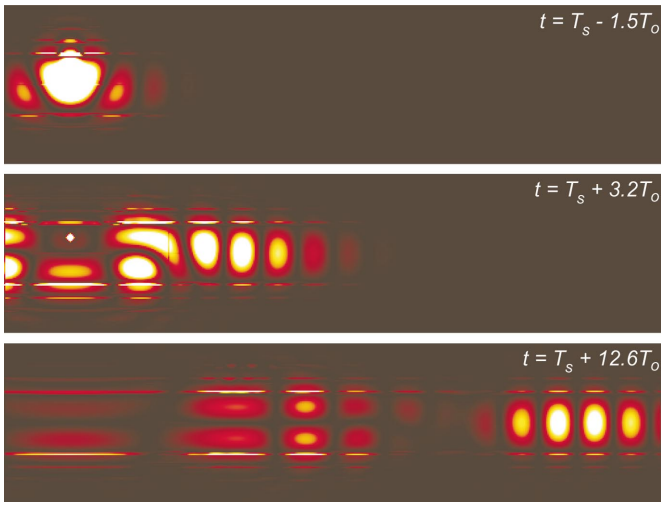

FIG. 14. (Color) Snapshots of the distribution of electrical power in the waveguide for a single-dipole source near the inner surface ($\rho = 1.2a$, $r_i = 2.144a$) pointing in the θ direction.

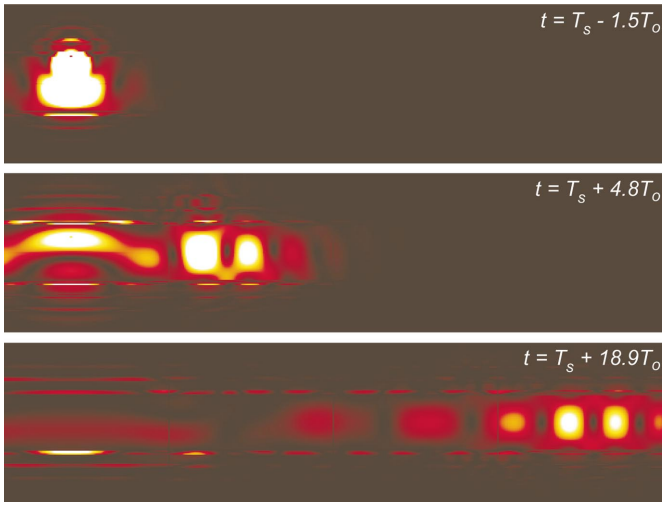

FIG. 15. (Color) Snapshots of the distribution of electrical power in the waveguide for a single-dipole source near the inner surface ($\rho = 1.2a$, $r_i = 2.144a$) pointing in the z direction.

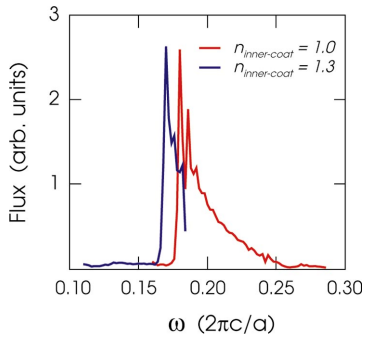

FIG. 16. (Color) Flux spectrum for dipoles oriented along z situated on inner wall of a medium-sized cell with an inner coating of low-index material ($n = 1.3$) extending from $\rho = 1.2a$ to $\rho = 2.144a$.

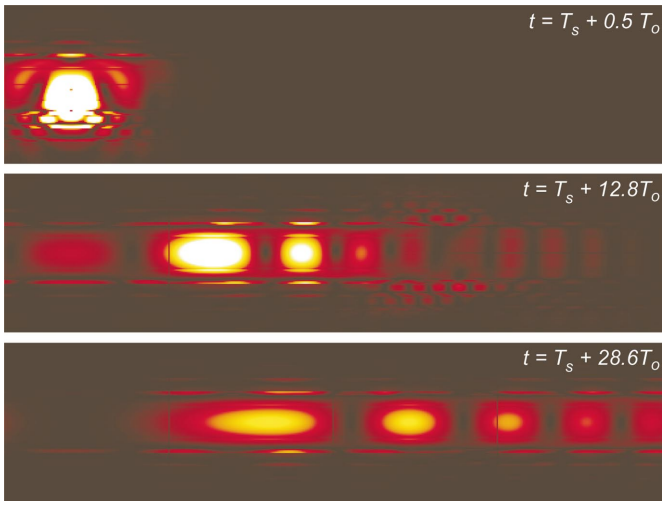

FIG. 17. (Color) Snapshots of the distribution of electrical power in the waveguide for a single-dipole source, oriented along z, on the inner surface of a cell with a coating of low-index material ($n = 1.3$) extending from $\rho = 1.2a$ to $\rho = 2.144a$.

hollow omniguide geometry are covered in some detail in Ref. 17. Applications of these principles to the detector application are briefly covered here. First, we consider the problem of choosing the appropriate mode. There are primarily TE-like and TM-like modes, which have an angular momentum m and index n. All properties of the TE modes can be calculated from $H_z = J_m(\omega\rho/c)e^{im\phi}$ subject to the boundary condition $\partial H_z/\partial\rho|_{\rho=R} = 0$ (where R is the core radius). Similarly, TM modes have a scalar E_z which vanishes at $\rho = R$. It has been shown that TE_{0n} mode losses scale as $1/R^3$, and all other mode losses scale as $1/R$. However, there are five modes with equal or lower cutoff frequencies as the TE_{01} mode, including several doubly degenerate modes. For simplicity, one may wish to restrict the fluorescent molecule to only couple to one mode. In this case, we choose the TM_{01} mode, which has a cutoff frequency of $\omega = 0.383/(r_i/a)$, where r_i is the inner-core radius. Only the TE_{11} mode has a lower cutoff frequency $[\omega = 0.293/(r_i/a)]$, though an emitter placed at the center can only couple to $m = 0$ modes (such as TM_{01}) due to the physical requirement that the fields be single valued. Alternatively, one could choose r_i to be small, for instance, $r_i = 2a$, so that the TE_{11} mode cutoff would be below the range of omnidirectional reflection, which would leave only the TM_{01} mode at the end of the omniguide. The last issue concerns choosing the appropriate number of cladding layers. The loss of a given mode for a given core radius and given number of layers can easily be calculated. For instance, a TM_{01} mode has a loss of 26 dB / cm for a radius of $6a$ and 4 bilayers of tellurium / polystyrene. If the target loss is 1 dB or less with a length of 1 cm of omniguide, the fact that TM losses decrease by a factor of 5 with each bilayer means that six cladding bilayers are needed.

IV. CONCLUSION

In conclusion, we have found that the radiation of dipole sources couples strongly into low-loss hollow-core guided modes of 1D periodic hollow omniguide structures. Furthermore, the rate of emission of these sources is controlled by the local density of states at its location and orientation. For states away from the inner surface there are 1D Van Hove singularities at the guided mode cutoff frequencies, just as in a metallic waveguide. This gives rise to spontaneous emission concentrated at frequencies just above cutoff, a substantial departure from the vacuum case. Strong modification of spontaneous emission has been already observed experimentally[22] for a metallodielectric photonic crystal. However, there is still the problem that sources near the inner surface can couple into guided modes in the dielectric cladding layers. Fortunately, this undesirable behavior can be reduced substantially through the introduction of a low-index coating on the inner surface of the hollow core.

[1] E. Marcatilli and R. Schmeltzer, Bell Syst. Tech. J. **43**, 1783 (1964).
[2] J. Harrington, Fiber Integr. Opt. **19**, 211 (2000).
[3] Y. Matsuura, T. Abel, and J. Harrington, Appl. Opt. **34**, 6842 (1995).
[4] M. Born, *Optik* (Springer, Berlin, 1933).
[5] W. Weinstein, J. Opt. Soc. Am. A **37**, 576 (1947).
[6] F. Abeles, Ann. Phys. **5**, 596 (1950); **5**, 706 (1950).
[7] M. Born and E. Wolf, *Principles of Optics* (Pergamon Press, Bath, England, 1959).
[8] P. Yeh, A. Yariv, and E. Marom, J. Opt. Soc. Am. A **68**, 1196 (1978).
[9] A. Cho, A. Yariv, and P. Yeh, Appl. Phys. Lett. **30**, 471 (1977).
[10] P. Yeh, A. Yariv, and C.-S. Hong, J. Opt. Soc. Am. A **67**, 423 (1977).
[11] N. Doran and K. Blow, J. Lightwave Technol. **LT1**, 588 (1983).
[12] M. Miyagi and S. Kawakami, J. Lightwave Technol. **LT2**, 116 (1984).
[13] C. de Sterke and I. Bassett, J. Appl. Phys. **76**, 680 (1994).
[14] Y. Fink, J.N. Winn, S. Fan, C. Chen, J. Michel, J.D. Joannopoulos, and E.L. Thomas, Science **282**, 1679 (1998).
[15] Y. Fink, D.J. Ripin, S. Fan, C. Chen, J.D. Joannopoulos, and E.L. Thomas, J. Lightwave Technol. **LT17**, 2039 (1999).
[16] M. Ibanescu, Y. Fink, S. Fan, E.L. Thomas, and J.D. Joannopoulos, Science **289**, 415 (2000).
[17] S. Johnson, M. Ibanescu, M. Skorobogatiy, O. Weisberg, T. Engeness, M. Soljacic, S. Jacobs, J. Joannopoulos, and Y. Fink, Opt. Express **9**, 748 (2001).
[18] S. Hart, G. Maskaly, B. Temelkuran, P. Prideaux, J. Joannopoulos, and Y. Fink, Science **296**, 510 (2002).
[19] B. Temelkuran, S. Hart, G. Benoit, J. Joannopoulos, and Y. Fink, Nature (London) **420**, 650 (2002).
[20] D. Kleppner, Phys. Rev. Lett. **47**, 233 (1981).
[21] R. Hulet, E. Hilfer, and D. Kleppner, Phys. Rev. Lett. **55**, 2137 (1985).
[22] J. Fleming, S. Lin, I. El-Kady, R. Biswas, and K. Ho, Nature (London) **417**, 52 (2002).
[23] K. Busch and S. John, Phys. Rev. E **58**, 3896 (1998).
[24] R. Magnanini and F. Santosa, SIAM (Soc. Ind. Appl. Math.) J. Appl. Math. **61**, 1237 (2000).
[25] K.S. Yee, IEEE Trans. Antennas Propag. **AP14**, 302 (1966).
[26] Z.S. Sacks, D.M. Kingsland, R. Lee, and J.-F. Lee, IEEE Trans. Antennas Propag. **AP43**, 1460 (1995).
[27] E. Purcell, Phys. Rev. **69**, 681 (1946).
[28] G. Gilat and L. Raubenheimer, Phys. Rev. **144**, 390 (1966).
[29] C. Hooijer, D. Lenstra, and A. Legendijk, Opt. Lett. **25**, 1666 (2000).
[30] G. Agrawal, *Applications of Nonlinear Fiber Optics*, Optics and Photonics (Academic Press, San Diego, CA, 2001).